

CFD predictions and comparisons with experimental data for a conducted hollow-cone spray

H. M. Abduljalil*, R. A. Sharief, A. J. Yule²

48 Heald Avenue, Manchester, M14 4HH, UK

² School of Computing, Science and Engineering, Salford University

Salford, Greater Manchester M5 4WT

Abstract

Detailed comparisons of *CFD* predictions using STAR-CD with experimental results of a hollow-cone spray obtained by using *PDA* system are presented here. This comparison study showed that the predicted distributions of mean droplet sizes were in reasonably good agreement with experimental results. Moreover, the predicted mean axial velocities of droplets showed good agreement with experimental results. The size/velocity correlations showed good agreement between the experimental data and *CFD* predictions for the shared range of drop sizes. The predicted influence of the spray on the entrained air matched the experimental data well.

Introduction

The objective of this study is to assess the capability of one *CFD* (Computational Fluid Dynamics) code for modelling the case of a hollow-cone spray conducted into a confinement tube with co-flowing airflow, by compare the predictions with experimental results. The experimental setup and results of [Abduljalil] are used for the current comparison studies. The commercial finite volume *CFD* code, STAR-CD version 3.100B, was used.

The liquid phase is modelled as a spray of discrete droplet parcels, each parcel containing many spherical, non-interacting droplets with the same size, velocity and temperature. By injection of sufficient of these droplet parcels the entire spray can be represented in a computationally efficient manner. The trajectories of the droplets are calculated by solving the Lagrangian equations. The gas phase is modelled using the Reynolds-averaged Eulerian continuum equations, and turbulence has been included via the standard *k-ε* model. Predictions of drop size, average drop velocity, and drop mass flux distributions are compared with experimental results obtained using *PDA* (Phase Doppler Anemometry) measurement system.

Model Structure

The spray has been modelled in a steady state manner, and due to the symmetry of the situation, the spray was modelled in a pseudo-two-dimensional manner. As shown in Figure 1, a cylindrical co-ordinate system grid was used with one 5° segment of cells where each of which with size of 2 mm in the radial [*r*] and axial [*x*] directions. The axis of the grid was modelled as a symmetry boundary and the outer boundary was modelled as a wall. The inlet plane was modelled with a constant uniform inlet air velocity of 12m/s, and the outlet plane was modelled using a “zero gradient” condition. The two side planes of the cell slice were modelled using symmetry boundary conditions.

The spray was injected on the grid axis 60mm from the inlet boundary, i.e. the exit orifice position of the atomizer. An area of cells 6mm x 60mm upstream of the injection point was removed from the grid to represent the presence of the atomizer and its holder as in the experimental setup.

As is usual in spray *CFD* models, primary atomization is not modelled due to the physical complexity of the processes involved. Instead droplet parcels are introduced to the model with properties so as to best represent the outcome of primary atomization. Due to the dense, fast spray produced near to the atomizer it is here very difficult to obtain droplet properties experimentally. Therefore, in this model experimental data obtained 25mm downstream from the atomizer have been used to represent the initial properties of the droplet parcels introduced to the model. An iterative method was used so that the droplet initial conditions have been refined by comparison of the model predictions at *x*=25mm with experimental data. The methodology to define the initial conditions for the spray drop sizes and velocities is introduced by [Abduljalil].

It is then assumed that the droplet parcels introduced to the model initially follow discrete trajectories (paths) such that the volume flux and the droplet sizes at *x* =25mm are correctly represented. The liquid volume flow rate associated with each of the above drop paths is provisionally calculated from the *PDA* volume flux data for *x*=25mm, assuming that each path corresponds to a region of $\pm\frac{1}{2}^\circ$ about the trajectory. These values are then normalised by dividing by the sum of the measured volume flow rates for each of the paths, and the corrected volume flow rates for each path were obtained by multiplying the normalised values with the actual atomizer volume flow rate. This procedure was necessary because the *PDA* technique is known to be unreliable quantitatively, whilst showing the correct shapes of paths.

* Corresponding author: hassan_abduljalil@yahoo.co.uk
Proceedings of the 21th ILASS - Europe Meeting 2007

The volume flow rates for each trajectory are used to calculate the number of droplets of each size to be introduced along each path. In general, for each drop size, a path had up to 100 parcels per second injected. For some drop paths close to the edge of the spray smaller numbers of parcels were introduced. The total numbers of parcels introduced to the model was 20,000.

The initial magnitude of absolute velocity of each droplet, at a given liquid injection pressure, is assumed to be the same. This is considered to be a reasonable assumption as the drops form from a liquid sheet which should have a uniform velocity across it shortly after it leaves the atomizer exit. These initial total velocities are divided into axial and radial components according to the initial angle of each drop path. The effect of atomizer dimensions on the velocity coefficient was studied by few workers like [Rizk and Lefebvre]. However, a velocity coefficient of 0.65 was chosen after making a few *CFD* runs (trials), not reported here, to check different values of velocity coefficient to best match the predictions of axial velocity profiles with the experimental data at the first measurement axial location.

The droplet parcels were initialized using the droplet parcels dialogue which specified the number of droplets per parcel, initial diameter, and liquid density and temperature. The droplet density, together with the diameter and the total number of droplets per parcel, as well as the total number of parcels, define the total mass of liquid injected during a given time. The velocity components were also introduced using the droplet parcels dialogue.

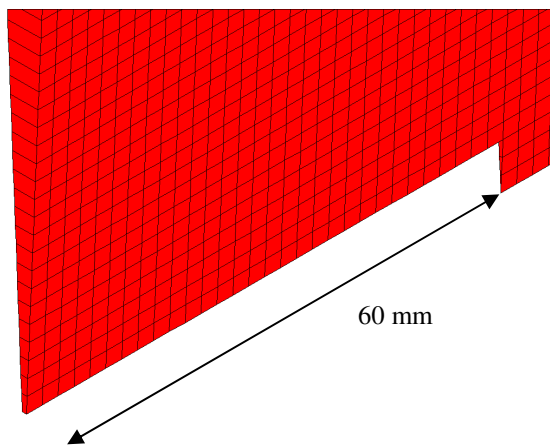


Figure 1: Grid structure used for modelling the confinement tube with magnified view showing the position of atomizer and its holder.

Results and Discussions

Figure 2 shows the experimental and predicted radial distributions in the confinement tube, of Sauter mean diameters for spray case at Liquid injection pressure of 2 MPa and co-flowing airflow velocity of 12 m/s. This figure shows that, in general, the model predictions match the trends of the experimental data, however there are differences when details are examined. The “winnowing” effect of the co-flowing air, which

separates the spray into narrower size distributions and fills the centre of the spray with smaller droplets, is not being well represented by the *CFD* results. It is recognised that errors in predictions of the downstream mean drop sizes profiles, could be due to inaccuracies in the prescribed size distribution at injection. However it is emphasised that the care taken over deriving these initial conditions was considerable, and exceeded that expected for normal users of the *CFD* code in industry, for example. The increase in mean drop size with distance downstream near the centreline of the spray in the experimental results has been attributed to the gradual entrainment of medium size droplets toward the centreline. However droplet collisions and coalescence might also have an effect.

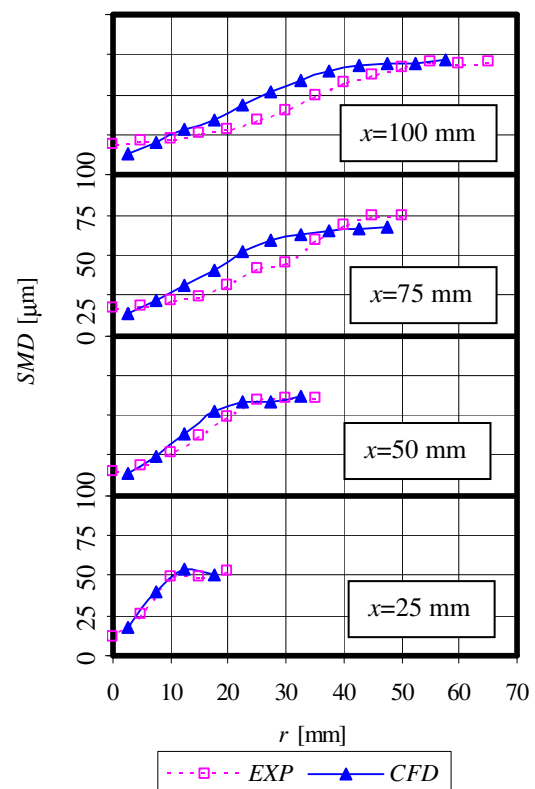


Figure 2: Predictions and experimental results of Sauter mean diameter (*SMD*) distributions at different downstream distances

The collision model was not used in these *CFD* models as it is only recommended for use for transient spray models [STAR-CD User’s Guide]. This could be proposed as an explanation of the discrepancy between the predicted and experimental mean diameters at the centreline of the spray. However, the spray densities are relatively low, typically 25×10^6 drops/m³ from the *PDA* data in the central zone, and thus significant coalescence should not occur. The cause of the discrepancy may also be an underestimation of the diffusion of the droplets across the tube. A comparison between the turbulence level intensities of the gas phase obtained from the *PDA* data and *CFD* predictions, not presented here because of

space limitation, showed an underestimation of turbulence level does occur in the predictions, which support this reasoning.

The reasonable matching of the predictions and experiments of spray width for the first three axial locations ($x \leq 50\text{mm}$) showed that there was no need to try other initial conditions and it is noted that an apparent underestimation, by the *CFD* model, of the diffusion of droplets by the turbulence would also have the effect of reduction of the width of the spray further downstream.

Drop size distributions (histograms) derived from the experimental data and the predictions at sample locations are presented in Figure 3. This figure shows that in parts (a) and (b) that close to the centre for spray the predictions have narrower size distributions than the measurements, with higher percentage of smaller droplets. For the zones between the centre and the outer part of the spray, Figure 3(c and d), predictions match measurements reasonably well.

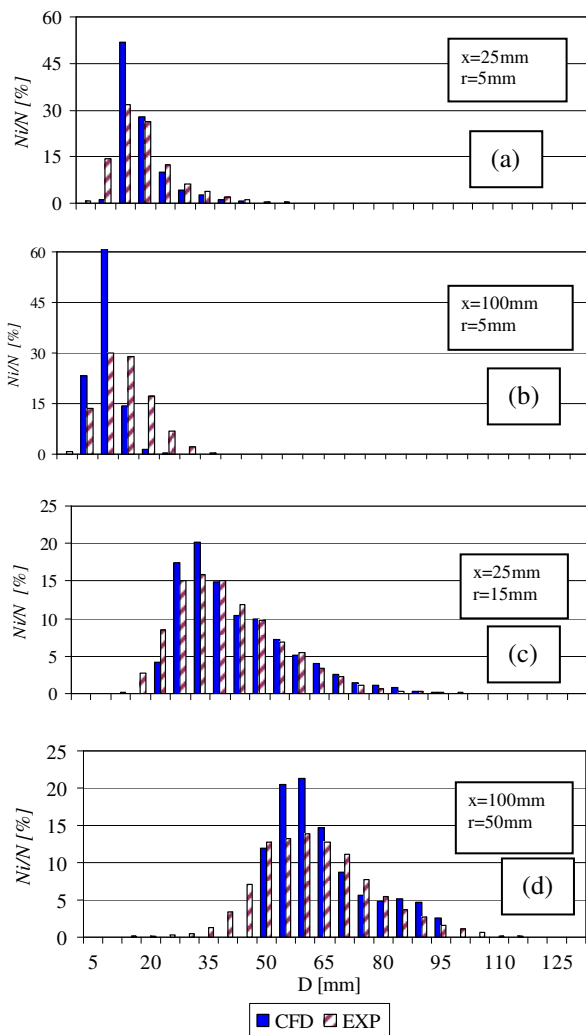


Figure 3: Comparisons between the experimental results and *CFD* predictions of drop size histograms, percentage in each size class of total number of drops is shown, first size class is $2.5\mu\text{m}$ to $7.5\mu\text{m}$.

Figure 4 shows comparisons of the experimental and predicted radial distributions of the mean axial droplet velocity component. This figure shows that the trends of the predicted velocity match the experimental data, with the radial profile decreasing in magnitude and increasing in uniformity with distance downstream. There is a tendency for the velocity near the centreline to be overpredicted, by typically 10%. This agreement is better than that for the mean droplet size profiles described in the section above. In particular the level of agreement at $x=25\text{mm}$ supports the validity of the initial velocity conditions that were specified for the model, including the value of velocity coefficient that has been used. The predicted and experimental positions of the peak velocity values at the outer part of the spray do not agree well. This is because these higher velocities correspond to larger droplets, which tend to congregate at the spray edges. As described above, the *CFD* model underpredicts the spreading rate. The predictions match the experimental data well further downstream where the droplets lose their momentum and move with a velocity very near to that of the co-flowing airflow.

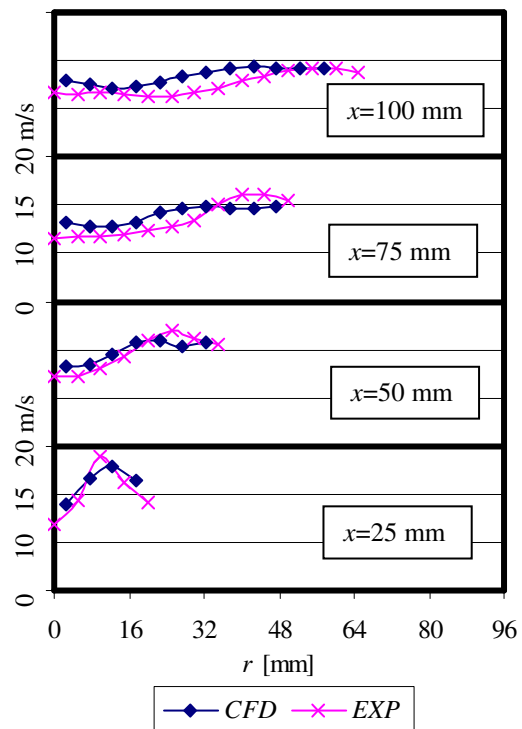


Figure 4: Predictions and experimental results of mean droplet axial velocity distributions

The size/velocity correlations at sample points at the first downstream axial location are presented and a comparison between the experimental data and *CFD* predictions is addressed. For experimental data, each point contains 10,000 samples. These comparisons are shown in Figure 5. Figure 5a shows that for the first downstream locations where $x = 50\text{mm}$, the experimental data and the *CFD* predictions show good matches of size/velocity correlations except for the

droplets with $D < 10 \mu\text{m}$. One can see that the lack of very small droplets ($D < 10 \mu\text{m}$) in predictions at x and r equal to 25 and 5mm respectively, does not lead to significant disagreement between the experimental data and *CFD* predictions of mean drop size at that point, due to the compensation by the higher percentage of predicted medium size droplets ($D = 15 \mu\text{m}$). Figure 5 shows also that size/velocity correlations at points near the edge of the spray ($r = 15\text{mm}$ at $x = 25\text{mm}$) match well for the shared range of drop sizes.

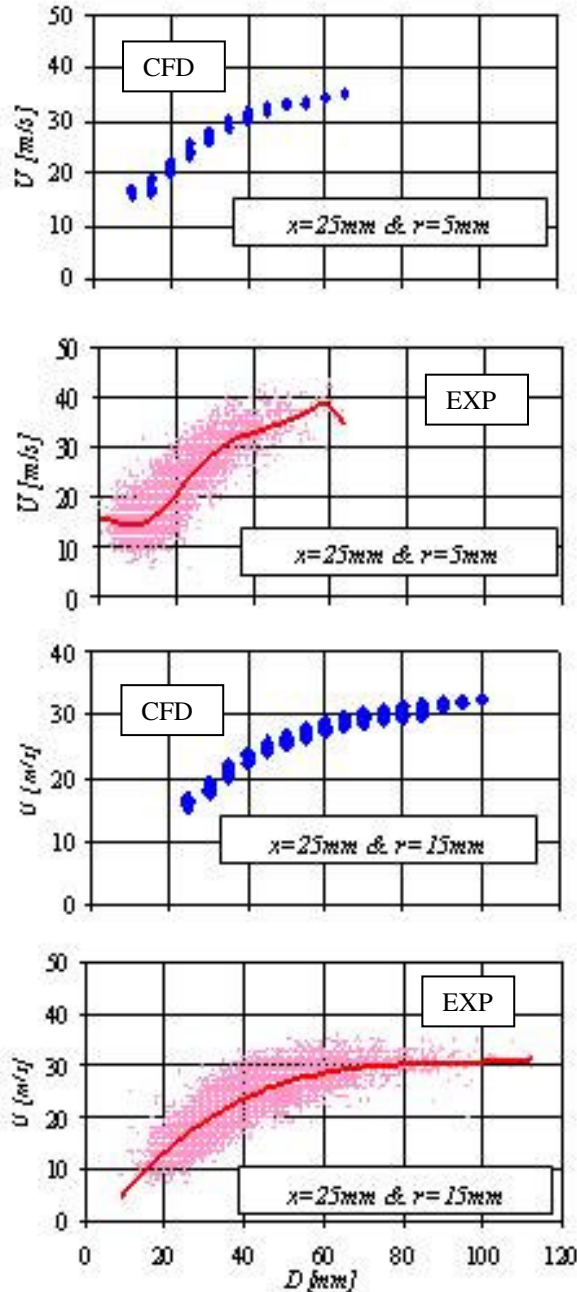


Figure 5: Size/velocity correlations, best fit 3rd or 4th polynomial curves shown for experimental cases

To enable comparison with *PDA* measurements of air velocity (from droplets with $D \leq 10 \mu\text{m}$) with and without sprays, the *CFD* model was also run for single

phase (no spray). The air velocity values were obtained from STAR-CD by defining “sensors” at the same downstream distances x as those used in *PDA* measurements. These “sensors” gave air velocity predictions at 1mm intervals in the radial direction. The mean air axial velocity profiles for cases with no spray is shown in Figure 6. This shows that, close to the atomizer, the wake of the atomizer and its holder body is wider in the experimental data than for the predicted results. This may be because the full geometry of the atomizer body and its holder could not be introduced to the model.

In order to fully model the atomizer and its holder body the situation should be modelled well upstream and with a finer mesh in the region of the holder, which was not possible in the current investigation due to limitation in computer power. As the effects of the atomizer wake vanish with downstream distance, the measured and predicted profiles become closer together and they coincide very well downstream. The predictions tend to overestimate the boundary layer thickness at the tube wall and this is possibly due to the need for more cells in this region.

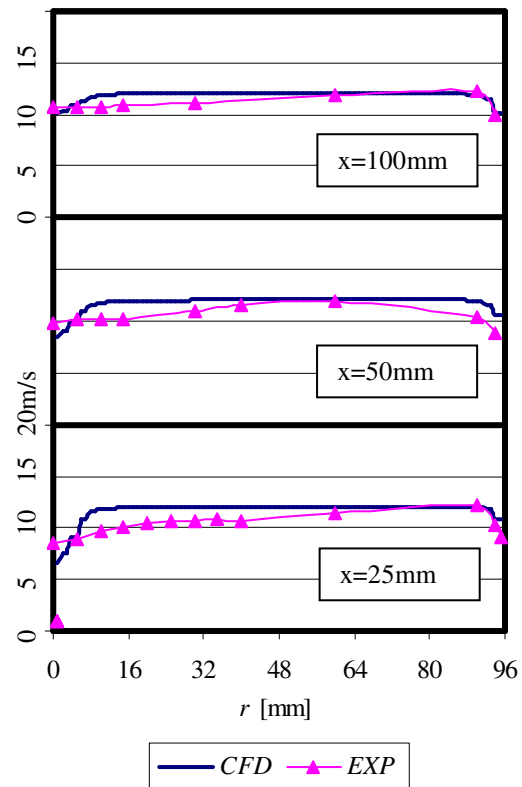


Figure 6: Predictions and experimental results of mean air axial velocity distributions, for no spray

The comparison of the predictions of the mean air axial velocity profiles with experimental results is shown in Figure 7. This figure shows that the predictions correctly show narrow jet-like flows at the centre of the tube, which are due to the entrainment of air by the sprays. However the predictions show peak values at the centre of the spray that are too high and

with too narrow widths for these zones. This could be influenced by the simplification in the modelling of the atomizer body as aforementioned.

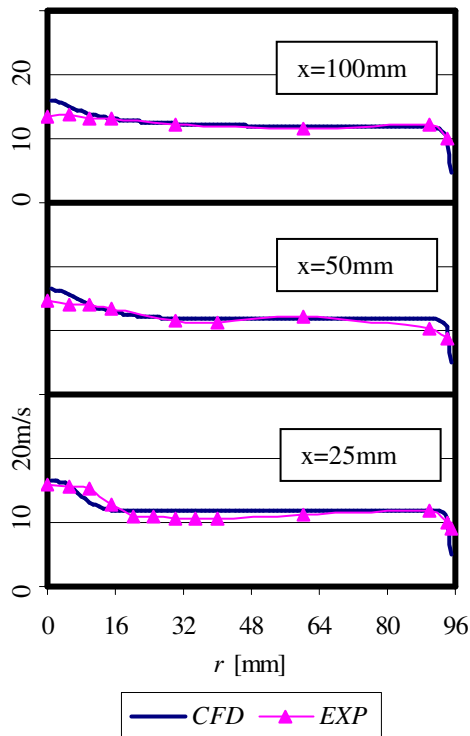


Figure 7: Predictions and experimental results of mean air axial velocity distributions

Comparisons between the predicted air velocity vectors, in the $x-r$ plane, for the cases with and without sprays show that the air flows outside the spray seems to be little affected by the spray when comparing the cases of air velocity with and without spray and it also shows the air being entrained into the spray toward the centreline. The experimental data of the axial velocity component also showed no observable difference between cases with and without sprays, outside the region of the spray envelope [Abduljalil]. It was not possible to measure the radial and axial velocity components simultaneously as the Dantec *PDA* system used in the current investigation is a “one-dimensional model”. It should be mentioned here that similar air velocity profiles, with central peaks of entrained air, were presented by [Widger] and [Dodge and Schwalb] both of whom used the FLUENT, commercial *CFD* code.

The predicted droplet volume flux distributions at different downstream axial locations of the spray case under investigation are shown in Figures 8. The volume flux was obtained using a developed code [Abduljalil] which calculates liquid volume flow rate in each grid cell and then, using an Excel worksheet, the volume flow rate is divided by the cross-sectional area of segments of the wedge of cells. The pattern of a hollow-cone spray is found initially with a low volume flux at the centre where small droplets are concentrated and

increasing values toward the edge of the spray to reach a peak value. This figure shows that the peak values of volume flux decrease with downstream distance x , as the spray spreads radially further downstream. These volume flux profiles show similar trends to those of the experimental data presented by [Abduljalil].

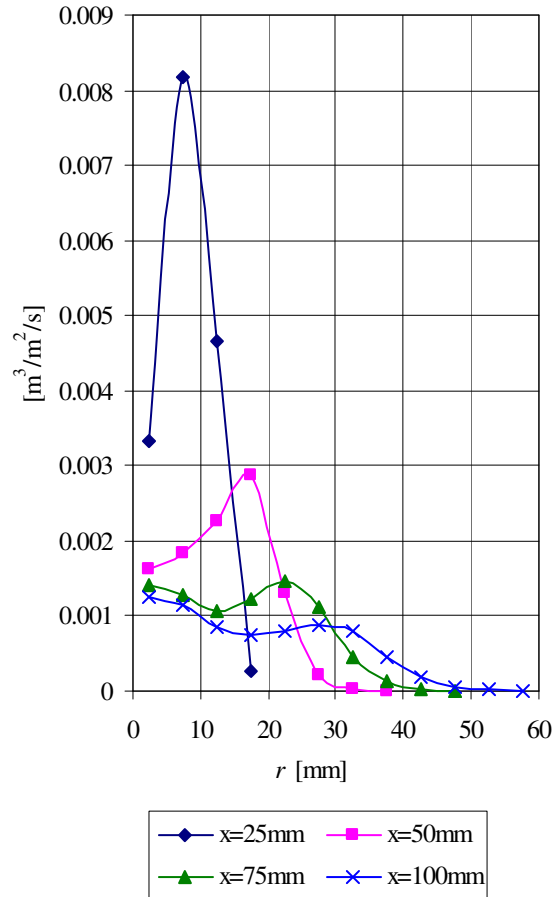


Figure 8: Predictions of volume flux distributions

Conclusions

There are significant problem areas (deficiencies) when using *CFD* codes to predict the characteristics of the sprays. One deficiency is in specifying the initial spray drop sizes and velocities with sufficient accuracy to compute spreading rates. In the current investigation a droplet initialisation method has been developed based on the experimental data at 25mm downstream of the atomizer exit. The STAR-CD code was used to model the confined sprays in co-flowing air flows and the lack of agreement with experiments for some of the results included errors in predicting droplet diffusion and the turbulence levels throughout the computational domain (the confinement tube).

The predicted distributions of mean droplet sizes were in reasonably good agreement with experimental results. The predicted mean axial velocities of droplets showed good agreement with experimental results, especially further downstream where all of the droplets lose their momentum and move with same velocity as

the air. The size/velocity correlations showed good agreement between the experimental data and *CFD* predictions for the shared range of drop sizes. The predictions showed narrower drop size distributions than the experimental data.

The predicted influence of the spray on the entrained air matched the experimental data well. The predictions showed that the air was entrained by the spray toward the centreline with almost no effect on the axial component of the mean air velocity outside the spray. The comparison between the experimental data and *CFD* predictions of the turbulence energy level along the confinement tube showed significant quantitative discrepancy where the *CFD* underpredicted the turbulence level in the computational domain even though it showed, generally, similar trends. The liquid mass (volume) flux showed a typical pattern for hollow-cone sprays. In addition, the amount of liquid stick at the wall of the tube showed, as expected, that the wider spray angle gave the higher deposition rate on the wall and the lower co-flowing air velocity gave higher deposition rate on the wall, for the same atomizer and liquid injection pressure.

References

1. H. M. Y. Abduljalil, An Experimental and Computational Study of Sprays Confined in a Tube, Ph. D. thesis, Department of Mechanical, Aerospace and Manufacturing Engineering, UMIST, Manchester, UK, 2003.
2. Anon, User Guide, STAR-CD v3.100B, Chapter 13, Computational Dynamics Ltd, London, 1999.
3. N. K. Rizk and A. H. Lefebvre, Prediction of Velocity Coefficient and Spray Cone Angle for Simplex Swirl Atomizer. *Proceedings of ICLASS-85*, pp. IIIC/2/1-IIIC/2/16, 1985.
4. R. Widger, Improvement of High Pressure Water Sprays Used for Coal Dust Extraction in Mine Safety, Ph. D. thesis, Mechanical Engineering Department, UMIST, Manchester, UK, 1993.
5. L. G. Dodge and J. A. Schwalb, Fuel spray evolution: comparison of experimental and CFD simulation of nonevaporating spray, *Journal for Engineering for Gas Turbine and Power*, Vol. 111, pp. 15-23, 1989.